The Journal of Experimental Biology 211, 606-612
Published by The Company of Biologists 2008
doi:10.1242/jeb.015115

Morphological and biochemical changes in the Harderian gland of hypothyroid rats

Rossella Monteforte[1], Alessandra Santillo[1], Antonia Lanni[1], Salvatore D'Aniello[2] and Gabriella Chieffi Baccari[1,*]

[1]Dipartimento di Scienze della Vita, Seconda Università degli Studi di Napoli, via Vivaldi, 43, 81100-Caserta, Italy and
[2]Department de Genetica, Facultat de Biologia, Universitat de Barcelona, Spain

*Author for correspondence (e-mail: gabriella.chieffi@unina2.it)

Accepted 11 December 2007

SUMMARY

The secretory activity of the Harderian gland (HG) is influenced by both exogenous (such as light and temperature) and endogenous (such as prolactin, thyroid hormones and steroid hormones) factors, which vary among species. In the present study, the effects of hypothyroidism on the rat HG were examined at morphological and biochemical levels. The decrease in cytoplasmic lipoproteic vacuoles and the increase in mucosubstance secretion in the acinar lumina were the most notable histological effects elicited by hypothyroidism. The release of all granules with nuclei and cellular debris suggested the occurrence of holocrine secretion. Electron microscopy revealed in the glandular cells of hypothyroid rat an increased condensation of chromatin in the nuclei, mitochondria with decreased cristae and vacuolisation, decreased glycogen granules, autophagic vacuoles, and lipofuscins in the cytoplasm. TUNEL reaction indicated DNA fragmentation in hypothyroid HG, indicative of an underlying apoptotic process. Translocation of cytochrome *c* from mitochondria to cytosol strongly supported this hypothesis. In conclusion, these findings indicate that thyroid hormones play a pivotal role in preserving the structural integrity of the rat HG and, hence, its secretory activity.

Key words: Harderian gland, ultrastructure, hormone action, hypothyroidism.

INTRODUCTION

The Harderian gland (HG) is an orbital gland present in most groups of terrestrial vertebrates. It is regulated by many exogenous and endogenous factors that vary according to the animal species (for reviews, see Payne, 1994; Chieffi et al., 1996). Numerous functions have been attributed to this gland, including lubrication of the eye and nictitating membrane, thermoregulation (Thiessen, 1988; Shanas and Terkel, 1996) and photoprotection (Hugo et al., 1987; Spike et al., 1990). Furthermore, it is part of the retinal–pineal axis (Hoffman et al., 1985) as well as a source of either pheromones or growth factors (Seyama et al., 1992; Shanas and Terkel, 1996). In some mammals, the HG activity is influenced by endogenous factors (such as prolactin, thyroid hormones and steroid hormones) and exogenous factors (such as light and temperature) (Hoffman et al., 1989a; Buzzell and Menendez-Pelaez, 1992; Buzzell et al., 1992; Menendez-Pelaez et al., 1993; Buzzell et al., 1994). During the 1940s, the interrelationship between the thyroid gland and the HG was suggested by several researchers (Smelser, 1943; Boas and Bates, 1954; Boas and Scow, 1954) who used glandular mass as their main study end point. These studies also suggested species differences: guinea pigs reacted to thyroidectomy with HG hypertrophy (Smelser, 1943) whereas the HGs of thyroidectomised rats decreased in mass (Boas and Bates, 1954). Decades later, thyroxine (T4) injections were found to hasten the appearance of new porphyrins in the HG of neonatal rats (Wetterberg et al., 1970). Recently, we demonstrated that 3,5,3′-triiodothyronine (T3) administration to adult rats induces HG hypertrophy (Chieffi Baccari et al., 2004). T4 injections lead to an increase in porphyrin content in female hamsters, an effect that is reversed under conditions of thyroid hormone deficiency (Hoffman, 1971; Hoffman et al., 1989a; Hoffman et al., 1989b; Hoffman et al., 1990). In addition, hypothyroidism induces a consistent increase in *N*-acetyl transferase (NAT) activity in male hamster HG (Buzzell et al., 1989) as well as in porphyrin levels (Hoffman et al., 1990). Furthermore, Hoffman and co-workers (Hoffman et al., 1990) have demonstrated that thyroid hormones act directly on the hamster HG rather than indirectly through modification of thyroid-stimulating hormone (TSH) synthesis and/or release. Nuclear receptors for T3 have been described in the HG of male and female golden hamsters (Vilchis and Pérez-Palacios, 1989). The presence of type II thyroxine 5′-deiodinase (5′D), an enzyme that converts thyroxine to triiodothyronine, in both rat and hamster HGs, provided further evidence that this gland is a target for thyroid hormones (Delgado et al., 1988; Osuna et al., 1990). Following thyroidectomy, the activity of 5′D in rat HG increases and exhibits a marked circadian rhythm (Guerrero et al., 1987). However, the effects of hypothyroid status on the morphofunctional characteristics of rat HG remain to be elucidated.

In this study, we investigated the effects of experimentally induced hypothyroidism on the morphology of rat HG by histochemistry and ultrastructural analyses. In addition, since we found that some morphological signs are indicative of cell death by apoptosis, we compared both mitochondrial and cytosolic expression of cytochrome *c* [the principal initiator molecule released from mitochondria to cytosol to initiate the apoptotic program in cells (Green and Reed, 1998)] in euthyroid and hypothyroid rat HGs.

MATERIALS AND METHODS

Animals and experiments

Male Wistar rats, *Rattus norvegicus albinus* Berkenhaut 1769, weighing 300–350 g, were kept under regulated conditions of temperature (28°C) and light (12 h:12 h L:D cycles). They received commercial food pellets (Mil-Rat, Morini, Italy) and water *ad libitum*. To induce hypothyroidism, rats (*N*=8) were injected intraperitoneally (i.p.) with 6-n-propylthiouracil (PTU) (1 mg 100 g^{-1} body mass) daily for 4 consecutive weeks. In addition, once a week, they received an i.p. injection of iopanoic acid (IOPA) (6 mg 100 g^{-1} body mass) (Lanni et al., 1996). Control rats (*N*=8) received saline injections. At the end of the treatment, rats were first anesthetised by an i.p. injection of chloral hydrate (40 mg^{-1} body mass) and then decapitated. The trunk blood was collected, and the serum was separated and stored at –20°C for later T3 and TSH determinations. The HGs were dissected out, weighed and rapidly immersed in liquid nitrogen for cytochrome *c* determination or for cryostat sectioning. Pieces of glands were quickly immersed in fixative for light or electron microscopy, as described below. Total T3 levels were determined in 50 μl samples of serum using reagents and protocols supplied by BD Biosciences (Franklin Lakes, NJ, USA). Serum TSH levels were measured by radioimmunoassay (RIA) using materials and protocols supplied by Amersham (Milan, Italy). Experiments were performed in accordance with local and national guidelines governing animal experiments.

Histology and histochemistry

Pieces of HGs were rapidly immersed in Bouin's fluid. Then, paraffin sections (5 μm thick) were stained with trichrome Mallory stain. A histochemical test for proteins was carried out using the mercury–Bromophenol Blue method, and the mucosubstances were

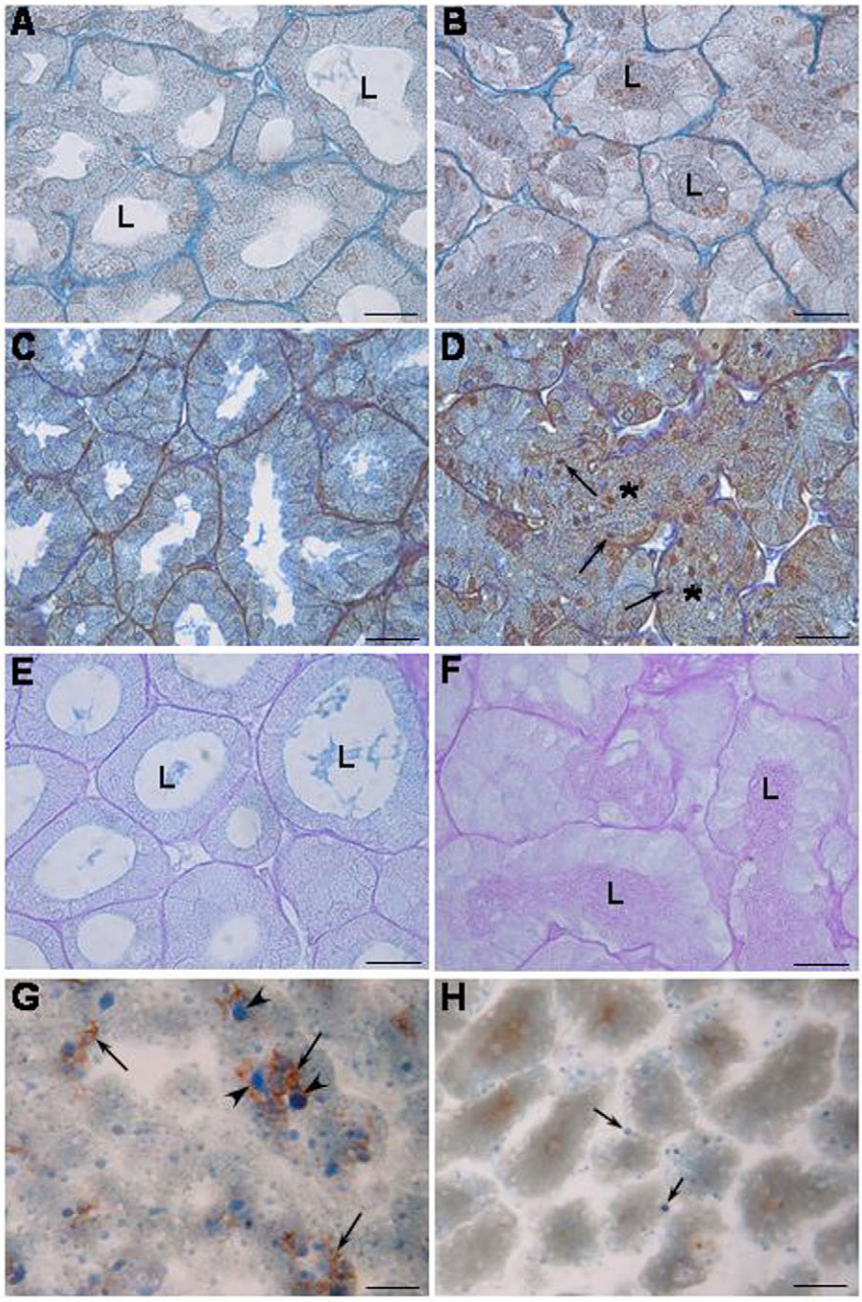

Fig. 1. Paraffin and cryostat sections of euthyroid and hypothyroid rat Harderian glands (HGs). (A) The glandular cells of euthyroid rat HG contain dense basophilic secretory granules and basal nuclei. L, lumen. (B) Glandular cells from hypothyroid rat HG show pale secretory granules. The acinar lumina (L) are filled with secretory granules mixed with nuclei and cytoplasmic fragments. A and B are Mallory stained. (C) The acinar cells from euthyroid rat HG are positive for the mercury–Bromophenol Blue reaction for protein. (D) In hypothyroid rat HG some glandular cells are weakly positive for the mercury–Bromophenol Blue reaction (blue stained), whereas the others are negative (brown stained). Pycnotic nuclei (arrows) can be observed. Acini coalescing can also be observed (asterisks). (E) The glandular epithelium of euthyroid rat HG is weakly positive for the AB/PAS reaction. L, lumen. (F) Glandular cells from hypothyroid rat HG are positive for AB/PAS reaction. The lumina (L) are filled with strongly positive AB/PAS secretion. (G) Cryostat section from euthyroid rat HG. Large Sudan Black-positive vacuoles (arrowheads) and porphyrin accretions (arrows) are present in glandular cells. (H) Cryostat section of hypothyroid rat HG. A few small vacuoles stained with Sudan Black are observed outside the acini (arrows). Scale bars, 16 μm.

detected with Alcian Blue–PAS (AB/PAS). For lipid detection, formol-calcium-fixed frozen sections (5–10 μm) were stained with Sudan Black B.

Ultrastructure

For electron microscopy, pieces of HGs (3 mm^3) were promptly immersed and left for 3 h in Karnovsky's fixative in cacodylate buffer (pH 7.4) and then postfixed for 2 h in cacodylate buffer containing 1% osmium tetroxide. The samples were dehydrated through a graded ethanol series and finally embedded in Epon 812. Ultrathin sections, stained with 4% uranyl acetate and then with 1% lead citrate, were examined using a Philips 301 transmission electron microscope (Philips Electronic Instruments, Rahway, NJ).

DNA nick end labelling of tissue sections

The terminal uridine deoxynucleotidyl transferase dUTP nick end labeling (TUNEL) reaction was performed on paraffin sections (5 μm thick) of HG using an *in situ* cell death detection kit (Roche Applied Science, Mannheim, Germany). Specifically, sections were pretreated with the permeabilisation solution (0.1% Triton X-100, 0.1% sodium citrate). Then, they were rinsed twice in PBS and incubated with a mixture containing terminal deoxynucleotidyl transferase (TdT) (1:20) and fluorescein-labelled dUTP, for 60 min at 37°C in a dark humidified chamber. After washing in PBS, the slides were examined under a fluorescence microscope.

Preparation of mitochondrial and cytosolic fractions

HG mitochondria were isolated after homogenisation in an isolation medium consisting of 220 mmol l^{-1} mannitol, 70 mmol l^{-1} sucrose, 20 mmol l^{-1} Tris–HCl, 1 mmol l^{-1} EDTA, 5 mmol l^{-1} EGTA, and 5 mmol l^{-1} MgCl2, pH 7.4 (all from Sigma-Aldrich Corp., St Louis, MO, USA), supplemented with a protease inhibitor cocktail (Roche Applied Science, Mannheim, Germany). After homogenisation, samples were centrifuged at 700 ***g*** for 10 min and supernatants were collected and transferred into new tubes for subsequent centrifugation at 17000 ***g***. The obtained mitochondrial pellet was washed twice and then resuspended in a minimal volume of isolation medium and kept on ice. The supernatant contained the cytosolic fraction (Singh et al., 2003).

Protein concentrations of mitochondrial and cytosolic fractions were estimated using a modified Bradford assay (Bio-Rad, Melville, NY, USA).

Western immunoblot analysis

Proteins from both mitochondrial and cytosolic fractions (30 μg each) were boiled in Laemmli buffer for 5 min. Afterwards, the samples were subjected to SDS–PAGE (13% polyacrylamide) under reducing conditions. Analysis of mitochondrial and cytosolic samples was performed on two separate gels. After electrophoresis, proteins were transferred to a nitrocellulose membrane. Each membrane was treated for 1 h with blocking solution (TBS/T: 5% non-fat powdered milk in 25 mmol l^{-1} Tris, pH 7.4; 200 mmol l^{-1} NaCl; 0.5% Triton X-100) and then it was incubated overnight at 4°C with a rabbit anti-human polyclonal antibody against cytochrome *c* (Cell Signalling Technology, Inc., Danvers MA, USA) diluted 1:1000. After washing with TBS/T and TBS, membranes were incubated with the horseradish-peroxidase-conjugated secondary antibody (1:4000) for 1 h at room temperature. The reactions were detected using a chemiluminescence protein detection method based on the protocol supplied with a commercially available kit (NEN Life Science Products, Boston, MA, USA). In both mitochondrial and cytosolic fractions, cytochrome *c* levels were determined using two preparations containing three glands from three different rats. The amount of cytochrome *c* protein was quantified by employing a Bio-Rad Molecular Imager FX using the supplied software (Bio-Rad Laboratories, Milan, Italy). The values obtained were compared by ANOVA followed by an unpaired *t*-test (for between-group comparison). All data were expressed as the mean ± s.d. The level of significance was set at $P<0.01$.

RESULTS

The combined effect of PTU and IOPA produced hypothyroid rats with T_3 levels significantly lower (0.13±0.02 nmol l^{-1}) than those observed in euthyroid rats (0.98±0.05 nmol l^{-1}). The serum TSH level was much greater in hypothyroid rats (20.1±1.2 mi.u. l^{-1}) than in euthyroid rats (4.3±0.4 mi.u. l^{-1}). HG mass was lower in hypothyroid rats (0.15±0.08 g) than in saline-injected rats (0.22±0.03 g).

Histology and histochemistry

The rat HG is a tubulo-alveolar gland surrounded by a connective tissue capsule. In the HG of euthyroid rats, the glandular epithelium had pyramidal cells with basal nuclei and large lumina (Fig. 1A). There are no morphological differences between the sexes in rat HG

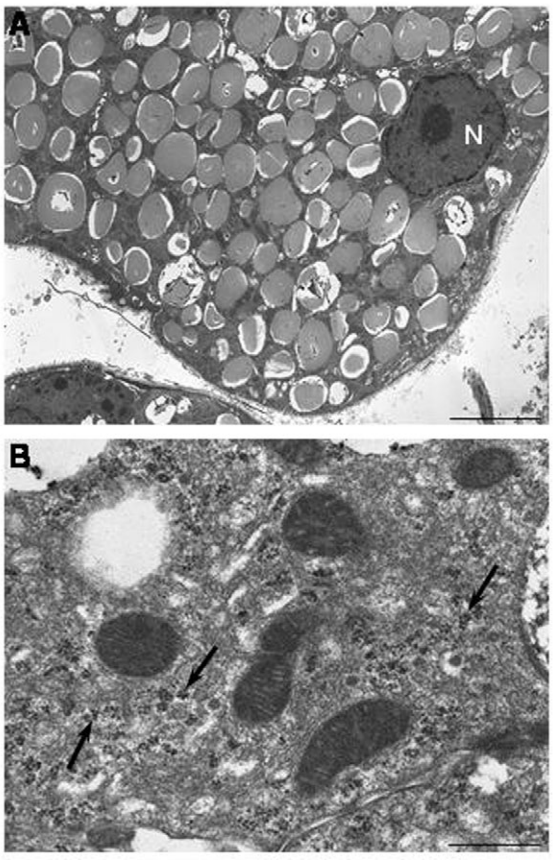

Fig. 2. Electron micrographs of type A cells from euthyroid rat Harderian gland (HG). (A) Large cytoplasmic vacuoles filled with moderately electron dense material occupy all the cytoplasm. The basal nucleus (N) has a prominent nucleolus. Scale bar, 7 μm. (B) Mitochondria with numerous tubular cristae and glycogen granules (arrows) are observed throughout the cytoplasm. Scale bar, 1 μm.

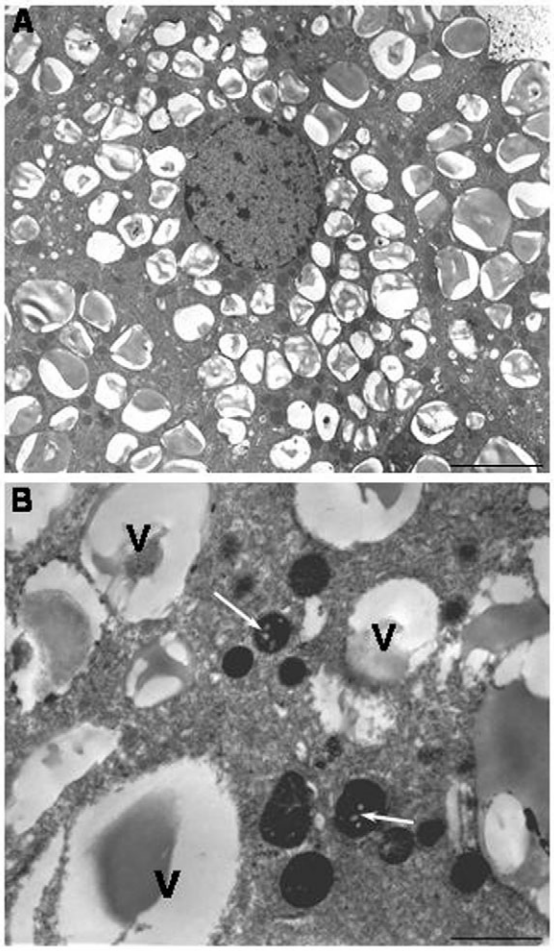

Fig. 3. Electron micrographs of type A cells from hypothyroid rat Harderian gland (HG). (A) Heterogeneous vacuoles almost devoid of secretory products can be seen throughout the cytoplasm. Scale bar, 5.4 μm. (B) Vacuolisations (arrows) are evident in the mitochondria, which are condensed. V, secretory vacuoles. Scale bar, 1.6 μm.

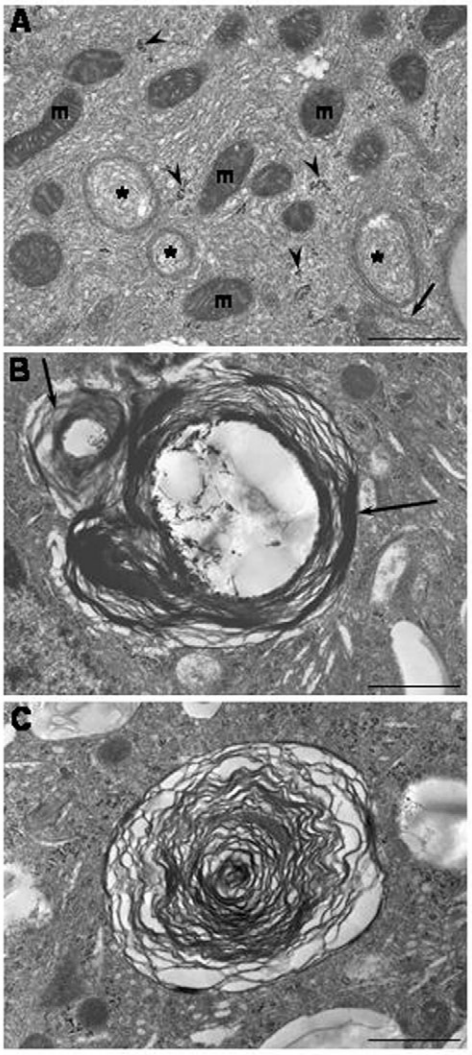

Fig. 4. Electron micrographs of type A cells from hypothyroid rat Harderian gland (HG). (A) Autophagic vacuoles (asterisks) can be seen close to smooth endoplasmic reticulum (arrow). Arrowheads indicate glycogen granules; m, mitochondria. Scale bar, 1.2 μm. (B) A cytoplasmic vacuole showing the characteristic lamellar substructures (arrows). (C) A secretory vacuole showing concentric systems of lamellae. Scale bars, 1 μm.

(for reviews, see Payne, 1994; Chieffi et al., 1996). We found that the morphology of the HG of hypothyroid rats (Fig. 1B) differed considerably from that of euthyroid rats (Fig. 1A). Indeed, the HG of hypothyroid rats was characterised by glandular cells that displayed pale secretory granules in the cytoplasm. Furthermore, the acinar lumina were filled with secretory granules mixed with nuclei and cytoplasmic fragments of glandular cells (Fig. 1B).

The acinar cells of euthyroid HG were positive for the Bromophenol Blue reaction (Fig. 1C) and weakly positive for the AB/PAS reaction (Fig. 1E). Large Sudan Black-positive vacuoles and porphyrin accretions were present in glandular cells of euthyroid HG (Fig. 1G). Glandular cells of hypothyroid rats were negative or weakly positive for Bromophenol Blue (Fig. 1D). The basal nuclei often appeared pycnotic. Some acini lost their normal structure and appeared detached from the extracellular matrix (Fig. 1D). Scarce connective tissue among acini was present. Coalescence of acini, as well as holocrine secretion, could be observed (Fig. 1D). Hypothyroid glandular cells were positive for AB/PAS and the lumina were filled with a strongly positive AB/PAS secretion (Fig. 1F). A few small Sudan Black-positive vacuoles were observed outside the acini (Fig. 1H).

Ultrastructure

As largely reported, two cell types are present in rat HG. Type A cells have large secretory vacuoles and type B cells have a few minute droplets (for reviews, see Payne, 1994; Chieffi et al., 1996). Electron micrographs revealed marked differences in the shape of glandular cells between euthyroid and hypothyroid rats. In euthyroid rats, type A cells (Fig. 2A) had a large number of cytoplasmic vacuoles containing a moderately electron-dense substance and basal nuclei with evident nucleoli. Numerous mitochondria with tubular cristae and glycogen granules were observed (Fig. 2B). In hypothyroid rats, type A cells had heterogeneously shaped cytoplasmic vacuoles (Fig. 3A). They were almost devoid of secretory products. Mitochondria with a few cristae often showed a condensed configuration and vacuolisation (Fig. 3B). A few glycogen granules were seen throughout the cytoplasm (Fig. 4A). Occasionally, bodies, interpreted as autophagic vacuoles, were observed (Fig. 4A). Some granules had

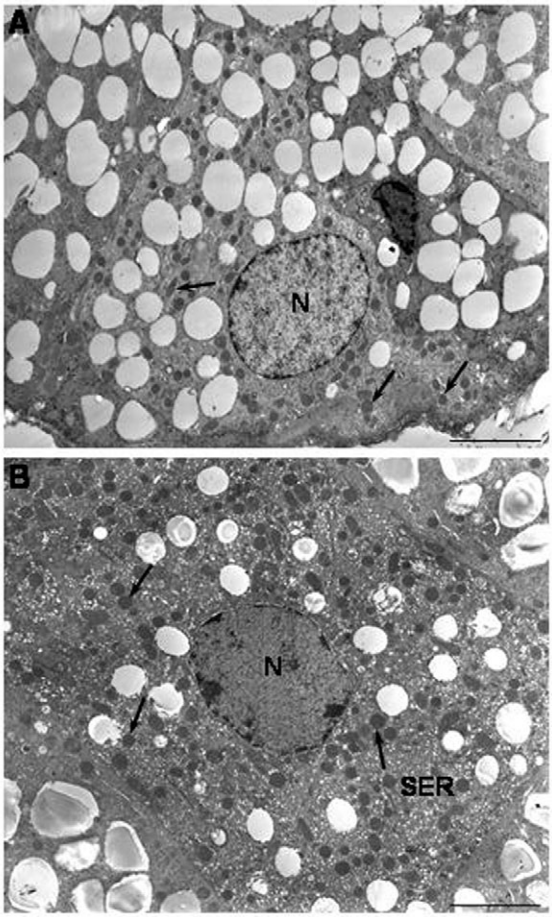

Fig. 5. Electron micrographs of type B cells from rat Harderian gland (HG). (A) Type B cells from euthyroid rat HG are characterised by cytoplasmic electron-translucent vacuoles and a basal nucleus (N). Numerous mitochondria (arrows) are observed throughout the cytoplasm. (B) Type B cells from hypothyroid rat HG have a dark nucleus (N) with peripheral condensation of chromatin and a few cytoplasmic vacuoles. Loose smooth endoplasmic reticulum (SER), as well as numerous mitochondria (arrows), can be observed throughout the cytoplasm. Scale bars, 5.4 μm.

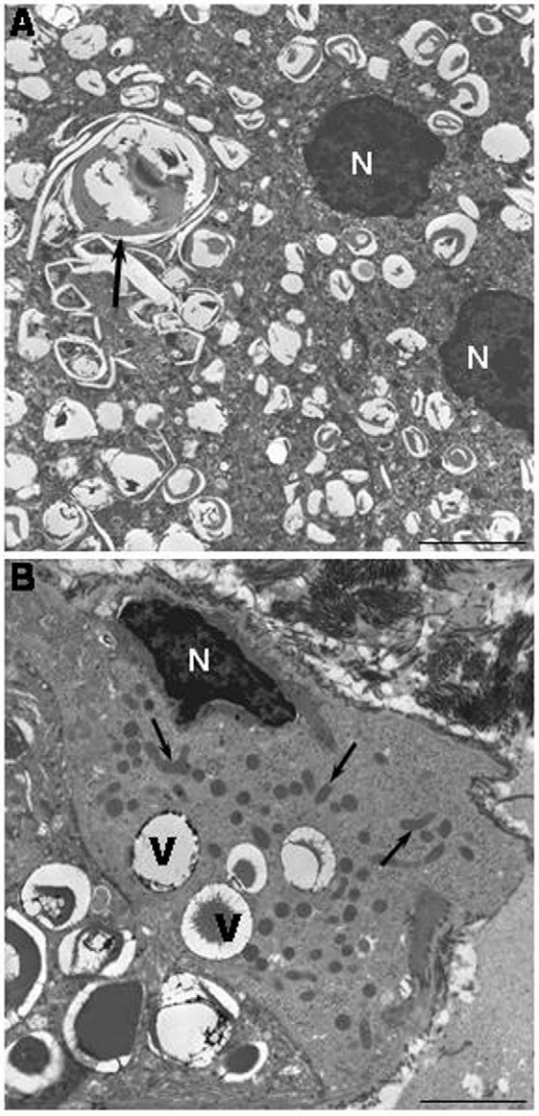

Fig. 6. Electron micrographs of hypothyroid rat Harderian gland (HG). (A) Type A cells have pycnotic nuclei (N) and heterogeneous secretory vacuoles throughout the cytoplasm. Coalescence of secretory vacuoles (arrow) can be seen. Scale bar, 5.4 μm. (B) Type A cells have a basal pycnotic nucleus and a few secretory vacuoles (V) throughout the amorphous cytoplasm. Arrows indicate mitochondria. Scale bar, 4 μm.

a characteristic lamellar substructure (Fig. 4B) and they often formed patterns resembling myelin forms (Fig. 4C).

Type B cells from euthyroid rat HG were characterized by empty cytoplasmic vacuoles and basal nuclei (Fig. 5A). Furthermore, these cells, compared to type A cells (Fig. 2A), had an abundant smooth endoplasmic reticulum (SER) and a larger number of mitochondria (Fig. 5A). In hypothyroid rats, type B cells had dark nuclei with peripheral condensation of chromatin and fewer cytoplasmic vacuoles than did euthyroid B cells (Fig. 5B). Loose SER, as well as numerous mitochondria, could be observed throughout the cytoplasm (Fig. 5B).

As shown in Fig. 6, some cells (types A and B) of the hypothyroid rat HG displayed strong signs of degeneration, including condensation of chromatin and pycnosis, profiles indicative of coalescence of secretory vacuoles (Fig. 6A), amorphous cytoplasm, and alteration of mitochondria (Fig. 6B).

DNA nick end labelling

Since we found morphological signs of cell degeneration in the HG from hypothyroid rats, we investigated apoptosis by the TUNEL technique. Whereas some nuclei from hypothyroid rat HG were labelled by fluorescein (Fig. 7A), the euthyroid HG nuclei were not (Fig. 7B).

Cytochrome *c* in mitochondrial and cytosolic fractions

Cytochrome *c* expression in mitochondrial and cytosolic fractions of euthyroid and hypothyroid rat HGs was compared. In the euthyroid state, the intensity of the cytochrome *c* band in the mitochondrial pellet was significantly ($P<0.01$) higher than that in cytosolic fraction (Fig. 8). Conversely, under hypothyroid conditions, the cytochrome *c* band was significantly more intense ($P<0.01$) in the cytosolic fraction than in the mitochondrial pellet (Fig. 8).

DISCUSSION

The combined treatment with PTU and IOPA produces rats with both systemic and local hypothyroidism. Indeed, PTU blocks

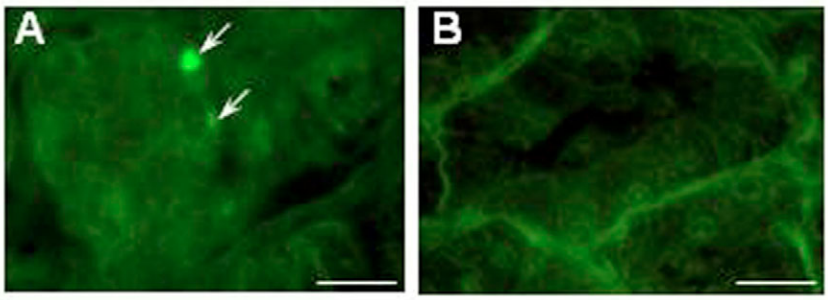

Fig. 7. TUNEL reaction in rat Harderian gland (HG). (A) Fluorescein-labelled nuclei (arrows) are observed in hypothyroid rat HG. (B) No fluorescence is present in the nuclei of euthyroid rat HG. Scale bars, 16 μm.

thyroidal hormone synthesis, *via* an inhibition of thyroid peroxidase activity and it is also a strong inhibitor of type I 5′-D-deiodinase activity (Oppenheimer et al., 1972; Leonard and Visser, 1986). IOPA inhibits all three types of deiodinase enzymes; however, whereas its effect is strong on type II and III, it is comparatively weak on type I (Kaplan and Utiger, 1978; St Germain, 1994). In the present study, the most notable histological effect of hypothyroidism in the rat HG was the decrease in cytoplasmic lipoproteic secretory granules and the increase in secretion in the lumina. The release of granules, together with cellular debris and some pycnotic nuclei in the lumina, suggests a holocrine type of secretion. This phenomenon was rarely observed in the HG of euthyroid animals in which merocrine secretion is prevalent (Woodhouse and Rhodin, 1963; Abe et al., 1980; Sakai, 1981; Satoh et al., 1992). Hence, the decreased weight of the HG in the hypothyroid condition could be ascribed to the massive release of glandular secretion. Consistently, we have previously demonstrated that the increased mass of the HG in hyperthyroid rats is due to the activation of the secretory activity induced by T3, which, indeed, provokes an accumulation of lipoproteic secretion into the cells and lumina (Chieffi Baccari et al., 2004).

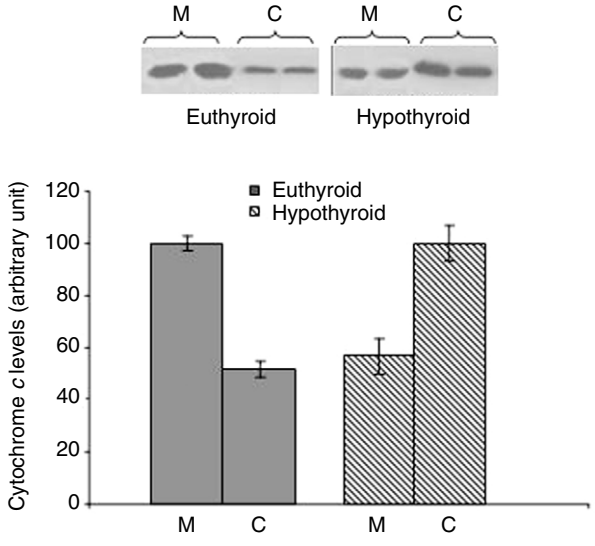

Fig. 8. Western blot detection of cytochrome *c* protein in mitochondrial and cytosolic fractions of euthyroid and hypothyroid rat Harderian gland (HG). In the euthyroid HG, the intensity of the cytochrome *c* band (14 kDa) in the mitochondrial pellet was significantly ($P<0.01$) higher than that in cytosolic fraction. Conversely, in hypothyroid HG, the cytochrome *c* band was significantly more intense ($P<0.01$) in the cytosolic fraction than in the mitochondrial pellet. Each mitochondrial and cytosolic preparations contained three glands from three different rats. C, cytosolic fraction; M, mitochondrial pellet.

Interestingly, although the rat HG secretes predominantly lipoproteic substances, histochemical tests revealed the presence of mucosubstances in the acinar lumina of hypothyroid rat HG, suggesting that under such conditions a biochemical modification of HG secretion takes place. An increase in the glycosaminoglycan content has been demonstrated in guinea pig HG after thyrotropin injections (Winand and Kohn, 1973). Therefore, mucosubstances accumulation in the HG of hypothyroid rats could be an effect of increased TSH serum levels.

The ultrastructural changes observed in hypothyroid rat HG could be attributed to the alterations in glandular activity elicited by thyroid hormone deficiency, thereby leading to eventual cell death. The electron microscopy revealed that in the final stages of cellular damage some cells had pycnotic nuclei and alterations in the cytoplasmic architecture without any accompanying swelling and rupture of nuclear and cytoplasmic membranes, indicative of necrosis. It is well known that cytochrome *c* is released from mitochondria in response to apoptotic stimuli (Green and Reed, 1998). We found cytochrome *c* translocation from mitochondria to the cytosol in hypothyroid rat HG. Hence, the alteration in mitochondrial morphology observed in hypothyroid rat HG may be due to the translocation of apoptogenic molecules. Consistently, as evidenced by TUNEL, DNA fragmentation in the gland of hypothyroid rat indicates the occurrence of apoptosis.

Interestingly, besides the occurrence of apoptosis in the hypothyroid rat HG, we also observed autophagic activity. Indeed, autophagic vacuoles and lipofuscins were detected and interpreted as the end result of autophagy. Our interpretation was based on recent studies describing an alternative pathways for active self-destruction called programmed cell death (PCD) type II or autophagy. Apoptosis, or PCD type I is characterised by condensation of cytoplasm and preservation of organelles, essentially without autophagic degradation. Autophagic cell death exhibits autophagic degradation of Golgi apparatus, polyribosomes, and endoplasmic reticulum, events that normally precede nuclear destruction (for a review, Bursch, 2001). Since apoptotic and autophagic PCD were are not mutually exclusive phenomena they could actually coexist in the hypothyroid rat HG. Autophagy has been recently described in hamster HG as a survival mechanism for fighting against cell damage resulting from physiological oxidative stress (Tomàs-Zapico et al., 2005).

Further studies are still needed to clarify the molecular mechanism underlying programmed cell death in rat HG under conditions of hypothyroidism. Although it is well known that thyroid hormone deficiency leads to extensive apoptosis during cerebellar development, the mechanisms by which it occurs still remain unclear. What is known is that thyroid hormones seem to preserve the mitochondrial architecture by inhibiting the release of apoptogenic molecules that can eventually lead to excess apoptosis

(Singh et al., 2003). Recently, a possible involvement of pro-nerve growth factor–p75 neurotrophin receptor pathway in hypothyroidism-enhanced apoptosis has been demonstrated during rat cortical development (Kumar et al., 2006). In addition, it has been demonstrated that hypothyroidism increases the level of p73, a protein involved in apoptosis, during rat liver regeneration (Alisi et al., 2005).

In conclusion, our findings indicate that the neuroendocrine–thyroid axis plays a pivotal role in preserving the structural integrity of rat HG and, therefore, its secretory activity. Without doubt, further studies are indispensable to clarify the mechanisms responsible for the morphological and biochemical changes in the HG and, consequently, the interplay between this gland and thyroid hormone deficiency.

LIST OF ABBREVIATIONS

AB/PAS	Alcian Blue–PAS
dUTP	uridine deoxynucleotidyl transferase
HG	Harderian gland
IOPA	iopanoic acid
PCD	programmed cell death
PTU	6-n-propylthiouracil
T_3	3,5,3′-triiodothyronine
TdT	terminal deoxynucleotidyl transferase
TSH	thyroid-stimulating hormone
TUNEL	terminal dUTP nick end labeling

We thank Mr Franco Iamunno for technical assistance and Dr Paola Merolla for the editorial revision of the manuscript.

REFERENCES

Abe, J., Sugita, A., Katsume, Y., Yoshizuka, M., Tamura, N., Iwanaga, S. and Nishida, T. (1980). Scanning electron microscopic observations of the harderian gland in rat. *Kurume Med. J.* **27**, 239-246.

Alisi, A., Demori, I., Spagnuolo, S., Pierantozzi, E., Fugassa, E. and Leoni, S. (2005). Thyroid status affects rat liver regeneration after partial hepatectomy by regulating cell cycle and apoptosis. *Cell. Physiol. Biochem.* **15**, 69-76.

Boas, N. F. and Bates, R. W. (1954). Role of the thyroid and anterior pituitary glands in the maintenance of the harderian glands of the rat. *Endocrinology* **55**, 601-612.

Boas, N. F. and Scow, R. O. (1954). Apparent exophthalmos in the rat following cortisone treatment or thyroidectomy. *Endocrinology* **55**, 148-155.

Bursch, W. (2001). The autophagosomal-lysosomal compartment in programmed cell death. *Cell Death Differ.* **8**, 569-581.

Buzzell, G. R. and Menendez-Pelaez, A. (1992). The interrelationship between the harderian glands and the neuroendocrine-thyroid axis in rodents. In *Harderian Glands: Porphyrin, Metabolism, Behavioral and Endocrine Effects* (ed. S. M. Webb, R. A. Hoffman, M. L. Puig-Domingo and R. J. Reiter), pp. 255-270. Berlin: Springer-Verlag.

Buzzell, G. R., Chen, Z., Vaughan, M. K. and Reiter, R. J. (1989). Effects of inhibition of thyroid function and of cold on melatonin synthesis and porphyrin content in the Harderian glands of male Syrian hamsters, *Mesocricetus auratus*. *Comp. Biochem. Physiol.* **94A**, 427-429.

Buzzell, G. R., Hoffman, R. A., Vaughan, M. K. and Reiter, R. J. (1992). Hypophysectomy prevents the castration-induced increase in porphyrin concentrations in the Harderian glands of the male golden hamster: a possible role for prolactin. *J. Endocrinol.* **133**, 29-35.

Buzzell, G. R., Menendez-Pelaez, A., Hoffman, R. A., Rodriguez, C. and Antolin, I. (1994). Androgenic control of porphyrin in the Harderian glands of the male Syrian hamster is modulated by photoperiod, which suggest that the sexual differences in porphyrin concentrations in this gland are important functionally. *Anat. Rec.* **240**, 52-58.

Chieffi, G., Chieffi Baccari, G., Di Matteo, L., d'Istria, M., Minucci, S. and Varriale, B. (1996). Cell biology of the Harderian gland. *Int. Rev. Cytol.* **168**, 1-80.

Chieffi Baccari, G., Monteforte, R., de Lange, P., Raucci, F., Farina, P. and Lanni, A. (2004). Thyroid hormone affects secretory activity and uncoupling protein-3 expression in rat harderian gland. *Endocrinology* **145**, 3338-3345.

Delgado, M. J., Guerrero, J. M., Santana, C., Menendez-Pelaez, A., Gonzalez-Brito, A., Chen, Z. L. and Reiter, R. J. (1988). Thyroxine 5′-deiodinase activity in brown adipose tissue, Harderian gland, pineal gland and pituitary gland of the male Syrian hamster (*Mesocricetus auratus*). *Neuroendocrinol. Lett.* **10**, 363-368.

Green, D. R. and Reed, J. C. (1998). Mitochondria and apoptosis. *Science* **281**, 1309-1312.

Guerrero, J. M., Puig-Domingo, M., Vaughan, G. M. and Reiter, R. J. (1987). Characterization of type II thyroxine 5′-deiodinase activity in rat Harderian gland. *Life Sci.* **41**, 1179-1185.

Hoffman, R. A. (1971). Influence of some endocrine glands, hormones and blinding on the histology and porphyrins of the Harderian glands of golden hamsters. *Am. J. Anat.* **132**, 463-478.

Hoffman, R. A., Johnson, L. B. and Reiter, R. J. (1985). Harderian glands of golden hamsters: temporal and sexual differences in immunoreactive melatonin. *J. Pineal Res.* **2**, 161-168.

Hoffman, R. A., Johnson, L. B., Vaughan, M. K. and Reiter, R. J. (1989a). Interaction of harderian glands, illumination, and temperature on thyroid hormones in golden hamsters. *J. Comp. Physiol. B* **158**, 697-702.

Hoffman, R. A., Wertz, P. and Habeeb, P. (1989b). Harderian glands of golden hamsters: morphological and biochemical responses to thyroid hormones. *J. Comp. Physiol. B* **159**, 293-299.

Hoffman, R. A., Habeeb, P. and Buzzell, G. R. (1990). Further studies on the regulation of the Harderian glands of golden hamsters by the thyroid gland. *J. Comp. Physiol. B* **160**, 269-275.

Hugo, J., Krijt, J., Vokurka, M. and Janousek, V. (1987). Secretory response to light in rat Harderian gland: possible photoprotective role of Harderian porphyrin. *Gen. Physiol. Biophys.* **6**, 401-404.

Kaplan, M. M. and Utiger, R. D. (1978). Iodothyronine metabolism in rat liver homogenates. *J. Clin. Invest.* **61**, 459-471.

Kumar, A., Sinha, R. A., Tiwari, M., Pal, L., Shrivastava, A., Singh, R., Kumar, K., Kumar Gupta, S. and Godbole, M. M. (2006). Increased pro-nerve growth factor and p75 neurotrophin receptor levels in developing hypothyroid rat cerebral cortex are associated with enhanced apoptosis. *Endocrinology* **147**, 4893-4903.

Lanni, A., Moreno, M., Lombardi, A. and Goglia, F. (1996). Calorigenic effect of diiodothyronines in the rat. *J. Physiol. Lond.* **494**, 831-837.

Leonard, J. L. and Visser, T. J. (1986). Biochemistry of deiodination. In *Thyroid Hormone Metabolism* (ed. G. Hennemann), pp. 189-229. New York: Marcel Dekker.

Menendez-Pelaez, A., Lopez-Gonzalez, M. A. and Guerrero, J. M. (1993). Melatonin binding sites in the Harderian gland of Syrian hamsters: sexual differences and effect of castration. *J. Pineal Res.* **14**, 34-38.

Oppenheimer, J. H., Schwartz, H. L. and Surks, M. I. (1972). Propylthiouracil inhibits the conversion of L-tlyroxine to L-triiodothyronine. *J. Clin. Invest.* **51**, 2493-2497.

Osuna, C., Rubio, A., Goberna, R. and Guerrero, J. M. (1990). Ontogeny of type II thyroxine 5′-deiodinase, N-acetyltransferase, and hydroxyindole-O-methyltransferase activities in the rat Harderian gland. *Life Sci.* **46**, 1945-1951.

Payne, A. P. (1994). The Harderian gland: a trecentennial review. *J. Anat.* **185**, 1-49.

Sakai, T. (1981). The mammalian Harderian gland: morphology, biochemistry, function and phylogeny. *Arch. Histol. Japan.* **44**, 299-333.

Satoh, Y., Ishikawa, K., Oomori, Y., Takede, S. and Ono, K. (1992). Secretion mode of the Harderian gland of rats after stimulation by cholinergic secretagogues. *Acta Anat.* **135**, 303-306.

Seyama, Y., Kasama, T., Yasugi, E., Park, S. H. and Kano, K. (1992). Lipids in Harderian glands and their significance. In *Harderian Glands: Porphyrin, Metabolism, Behavioral and Endocrine Effects* (ed. S. M. Webb, R. A. Hoffman, M. L. Puig-Domingo and R. J. Reiter), pp. 195-217. Berlin: Springer-Verlag.

Shanas, U. and Terkel, J. (1996). Grooming secretions and seasonal adaptations in the blind mole rat (*Spalax ehrenbergi*). *Physiol. Behav.* **60**, 653-656.

Singh, R., Upadhyay, G. and Godbole, M. M. (2003). Hypothyroidism alters mitochondrial morphology and induces release of apoptogenic proteins during rat cerebellar development. *J. Endocrinol.* **176**, 321-329.

Smelser, G. K. (1943). Changes induced in the Harderian gland of the guinea pig by the injection of hypophyseal extracts. *Anat. Rec.* **86**, 41-57.

Spike, R. C., Payne, A. P., Thompson, G. G. and Moore, M. R. (1990). Porphyrin profiles in hamster Harderian glands. *Biochem. Soc. Trans.* **18**, 630-631.

St Germain, D. L. (1994). Biochemical study of type III iodothyronine deiodinase. In *Thyroid Hormone Metabolism, Molecular Biology and Alternative Pathways* (ed. S. Y. Wu and T. J. Visser), pp. 45-66. Boca Raton: CRC Press.

Thiessen, D. D. (1988). Body temperature and grooming in the Mongolian gerbil. *Ann. N. Y. Acad. Sci.* **525**, 27-39.

Tomàs-Zapico, C., Caballero, B., Sierra, V., Vega-Naredo, I., Alvarez-Garcia, O., Tolivia, D., Rodriguez-Colunga, M. J. and Coto-Montes, A. (2005). Survival mechanisms in a physiological oxidative stress model. *FASEB J.* **19**, 2066-2068.

Vilchis, F. and Pérez-Palacios, G. (1989). Steroid hormone receptors and the sexual phenotype of the Harderian gland in hamster. *J. Endocrinol.* **112**, 3-8.

Wetterberg, L., Yuwiler, A., Geller, E. and Shapiro, S. (1970). Harderian gland: development and influence of early hormonal treatment on porphyrin content. *Science* **168**, 996-998.

Winand, R. J. and Kohn, L. D. (1973). Retrobulbar modifications in experimental exophthalmos: the effect of thyrotropin and an exophthalmos-producing substance derived from thyrotropin on the $^{35}SO_4$ incorporation and glycosaminoglycan content of harderian glands. *Endocrinology* **93**, 670-680.

Woodhouse, M. A. and Rhodin, J. A. G. (1963). The ultrastructure of the Harderian gland of the mouse with particular reference to the formation of its secretory product. *J. Ultrastruct. Res.* **9**, 76-98.